Structure-Directing Agent Location and Non-Centrosymmetric Structure of Fluoride-Containing Zeolite SSZ-55

Allen Burton,[†] Richard J. Darton,[‡] Mark E. Davis,[§] Song-Jong Hwang,[§] Russell E. Morris,*[,‡] Isao Ogino,[§] and Stacey I. Zones[†]

ChevronTexaco Energy Research and Technology Company, Richmond, California 94802, EaStCHEM School of Chemistry, University of St. Andrews, Purdie Building, St. Andrews KY16 9ST, U.K., and Department of Chemical Engineering, California Institute of Technology, Pasadena, California 91125

Received: September 1, 2005; In Final Form: January 9, 2006

Single crystals of pure silica zeolite SSZ-55 were prepared using the fluoride route. Single-crystal X-ray diffraction at a synchrotron source revealed the framework structure of the material, but the unit cell (orthorhombic $a = 12.905(2)$ Å, $b = 21.344(4)$ Å, $c = 5.1279(10)$) is too small to accommodate ordered arrays of the organic structure-directing agent. Molecular modeling was used to simulate the docking of the structure-directing agent in the channels of the material, and this revealed a strong space-filling interaction with a number of possible orientations of the organic cation. The overall non-centrosymmetric structure of the solid (spacegroup $C222_1$) was confirmed using second harmonic generation experiments.

Introduction

Zeolites are crystalline solids with channels and voids of similar dimensions to small organic molecules. Their chemical properties combined with their structural architecture lead to many applications in catalysis, ion exchange, and gas adsorption, and they also have potential in many emerging applications in optoelectronics, medicine, etc.[1] Pure silica zeolites are generally prepared in two different ways under hydrothermal conditions: at high pH in the presence of hydroxide (OH^-) ions or at lower pH in the presence of fluoride (F^-) ions using a method that was pioneered by Flanigen and Patton.[2] Aluminophosphate materials, which are isoelectronic with pure SiO_2 materials, can also be prepared with fluoride ions present, usually at near-neutral conditions.[3] The choice of these so-called mineralizers can have a profound influence on the particular solid formed. For high-silica zeolites, the major advantages of the fluoride route is that the solids are relatively defect-free,[4] they are generally low density, and they can be grown as quite large crystals.[5] The fluoride route has developed into one of the most productive methods for new materials, with some of the most interesting and promising zeolites of recent times resulting from this synthesis technique.[6−8]

Camblor and co-workers have postulated that fluoride ions perform two main functions during the formation of the silicate-based zeolite: a mineralizing role in improving the solubility of silicate ions at neutral pHs and a catalytic role in the formation of Si−O−Si bonds.[9] Often (but not exclusively) the presence of fluoride is a determining factor in which zeolite framework is crystallized, and one can therefore also add a tentative structure-directing role to its list of functions.[10]

It is also clear that the fluoride ions are often incorporated into many of the zeolite and aluminophosphate structures, balancing the positive charge of organic structure-directing cations that are also incorporated into the 'as-made' structures. Koller and co-workers, using solid-state NMR spectroscopy, have shown that the fluoride ions are connected to the framework, forming five-coordinated $SiO_{4/2}F^-$ units.[11,12] The fluoride ions therefore introduce a negative charge onto the framework itself. In contrast to other methods of introducing the required negative charge, such as aliovalent replacement of silicon with Al^{3+} ions or the introduction of connectivity defects, the fluoride ions are often ordered in specific sites. Single-crystal X-ray diffraction of pure silica zeolites prepared by the fluoride method indicate that the F^- ions tend to reside inside small cages[13−16] and are usually connected to a silicon atom that is part of a four-membered ring (i.e., a ring containing four silicon atoms). Depending on the structure and the conditions, the fluoride ion can be connected to one silicon atom in particular or disordered over a number of sites inside the same small cage, and this disorder may be static or dynamic depending on the specific zeolite structure and the temperature at which the observations are made.[17]

Apart from its use to produce novel materials, perhaps the most interesting observation in recent years is that as-made zeolite IFR, prepared using the fluoride method, shows non-centrosymmetric and polar ordering even though the calcined zeolite framework is centrosymmetric.[18] Clearly, this opens up a new structural role for the negatively charged fluoride ions. Polar solids show a number of interesting macroscopic properties, including optical nonlinearity (NLO), pyroelectricity, piezoelectricity, etc., and this has led to numerous attempts to incorporate interesting organic molecules inside the pores and cavities of zeolites and other microporous materials[19] and to supramolecular channel inclusion compounds.[20] The major advantage of zeolite-based materials is the combination of inorganic frameworks with dipolar organic molecules to produce very robust functional materials with many potential applications. A major obstacle to this work is the need for the final material to crystallize in a non-centrosymmetric spacegroup in order to be an active NLO or pyroelectric material.

Here we describe a study of as-made zeolite SSZ-55 prepared using the fluoride method and structurally investigated using

* To whom correspondence should be addressed. E-mail: rem1@st-and.ac.uk.
[†] ChevronTexaco Energy Research and Technology Company.
[‡] University of St. Andrews.
[§] California Institute of Technology.

10.1021/jp054950o CCC: $33.50
Published on Web 02/24/2006

single-crystal X-ray diffraction at a synchrotron source. The material reported here is the first to be prepared using a structure-directing cation that contains fluorine and fluoride ions as the mineralizer in the preparation. This material has the framework topology designated by the ATS code[21] with maximum symmetry *Cmcm*. However, the real symmetry of the archetype aluminophosphate is monoclinic *C*2/*c*.[22] Similarly, the calcined version of borosilicate SSZ-55, solved from powder X-ray diffraction data using the ZEFSAII algorithm, was reported in spacegroup $Cmc2_1$.[23] In this study we report the synthesis and single-crystal X-ray determination of as-made silica SSZ-55. The spacegroup is again reported as non-centrosymmetric, in this case $C222_1$. The structure-directing agent (SDA) used in the synthesis of this material **1** is too large to be accommodated in the unit cell of the material and so must be disordered and cannot be located by XRD. Docking calculations were therefore used to determine the location of the SDA in the material.

Experimental Section

Synthesis. A Teflon cup for a Parr 23 mL reactor was tared, and then 9.6 g of a solution of the SDA ([(1-(3-fluorophenyl)-cyclopentyl)methyl] trimethylammonium hydroxide, **1**) was

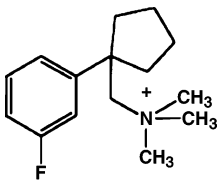

1

added into the cup (5 mmol). Next, 2.08 g of tetraethyl orthosilicate was added into the cup (10 mmol of SiO_2), and the open cup was placed in a hood and allowed to evaporate (loss of ethanol and water) until appearing to be dry after several days. Then the cup was re-weighed, and additional water added back in to adjust the H_2O/SiO_2 ratio to 10. Then 0.192 g of 48−52 wt % HF was added and the system stirred with a plastic spatula until a stiff gel had formed.

The Teflon cup was closed and sealed in the stainless steel reactor and was then placed onto a spit which rotates at 43 rpm within a Blue M convection heating oven. The oven had been set at 423 K. The reactor was taken out every 6 days, and a small sample was removed for analysis by scanning electron microscopy (Hitachi S-570 model). After the sample was heated for 30 days, the large crystals used in this study were seen in the field, and the product was collected and washed on a glass filter. The sample was then analyzed by powder X-ray diffraction and shown to be zeolite SSZ-55. Carbon-13 and ^{19}F MAS NMR spectra confirm that the template is intact in the structure and that fluorine is present, respectively (see Supporting Information).

Single-Crystal X-ray Diffraction. The crystals were generally of good quality (Figure 1) when viewed through a polarizing microscope. A crystal with a maximum dimension of about 60 μm was chosen for the diffraction experiment, and diffraction data were collected at the Daresbury Synchrotron Radiation Source using X-rays of wavelength 0.6897 Å (Silicon 111 monochromator) on a Bruker-Nonius goniometer equipped with a 1K CCD area detector. The temperature was held at 150 K.

A reasonably good quality intensity data set was collected ($R_{int} = 0.0256$), and normal structure solution followed. Details of the structure solution and refinement are given in Table 1. Structure solution was carried out using the program SHELXS-97 and least-squares refinement using the program SHEXL-97. The structure was solved using the normal procedures, with all the framework atoms found from the Direct Methods and from subsequent difference Fourier syntheses.

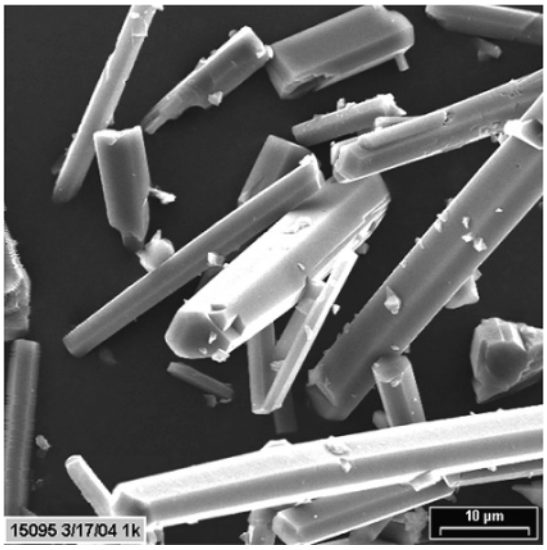

Figure 1. Scanning electron micrograph of the crystals of SSZ-55.

TABLE 1: Crystal Data and Structure Refinement for As-Made SSZ-55[a]

temperature	150(2) K
wavelength	0.6870 Å
crystal system, space group	orthorhombic, $C222_1$
unit cell dimensions	$a = 12.905(2)$ Å
	$b = 21.344(4)$ Å
	$c = 5.1279(10)$ Å
volume	1412.4(5) Å^3
θ range for data collection	1.84−29.47°
limiting indices	$-18 \le h \le 17$, $-23 \le k \le 30$, $-7 \le l \le 7$
reflections collected/unique	5064/1963 [R(int) = 0.0256]
refinement method	full-matrix least-squares on F^2
data/restraints/parameters	1963/6/118
goodness-of-fit on F^2	1.39
final R indices [$I > 2\sigma(I)$]	$R_1 = 0.076$, $Rw_2 = 0.223$
largest diff. peak and hole	2.8, −0.7 e·A^{-3}
goodness-of-fit on F^2[b]	1.07
final R indices [$I > 2\sigma(I)$][b]	$R_1 = 0.039$, $Rw_2 = 0.108$
largest diff. peak and hole[b]	0.50, −0.46 e·A^{-3}

[a] SDA not included in the refinement. [b] After use of the Squeeze program to remove electron density that occurs because of scattering resulting from unmodeled SDA molecules in the pores of the zeolite.

Molecular Modeling. The molecular modeling calculations were performed with the Cerius2 software from SGI (now Accelerys). The Burchart-Universal force-field was used for the energy minimization calculations of the SDA within the void space of the zeolite framework. Only van der Waals and intramolecular interactions were considered. Coulombic interactions were neglected during the optimization procedure, and the extraframework fluorine atoms were not included in the calculations. The zeolite framework was held fixed during the docking procedure, and several initial configurations of the molecule were exhaustively sampled within the zeolite void space. Supercells of two and three unit cells in length along the pore axis were created to allow sufficient space and optimal sampling of the relative configurations of neighboring SDA molecules. The reported optimization energies are the differences in the energy of the optimized free molecule and the global minimum energy of the molecule occluded within the framework.

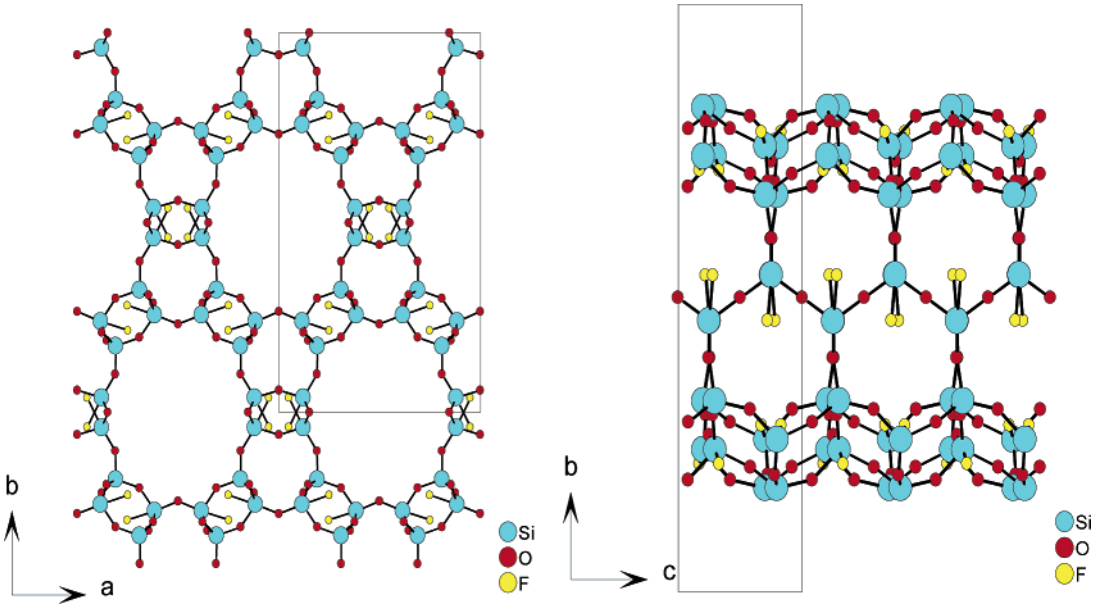

Figure 2. Two views of the framework structure of as-made SSZ-55 illustrating the location of the fluoride ions (yellow spheres).

Second Harmonic Generation (SHG). SHG measurements were accomplished using and Nd:YAG laser (1060 nm), and frequency doubled response was measured using a photomultiplier. Samples were prepared by grinding to a fine powder and mounted between two thin sheets of Mylar, which were then clamped between two microscope slides and clamped in the path of the laser beam. A reference of potassium titanyl phosphate (KTP) was used as a rough comparison of the strength. No attempt was made to quantify the SHG signal, and so the results presented below indicate only the presence or absence of a signal, indicating whether the sample is likely to be non-centrosymmetric or not.

Results and Discussion

Analysis of the systematic absences identified the spacegroup unambiguously as $C222_1$. The non-centrosymmetric nature of the material was confirmed by the observation of a positive second harmonic generation response on exposure to a Nd:YAG laser beam. While this SHG response is relatively weak when compared to the standard sample (KTP), it is still clearly strong enough to be a bulk effect (and not a result of surface effects); for this response to be seen, the structure has to be non-centrosymmetric.[24] The location and refinement of the silicon and oxygen atoms of the framework from the XRD data was successful. Refinement of the anisotropic displacement parameters (ADPs) revealed some large values for some of the oxygen atoms, which are probably due to static disorder caused by the SDA (see below). A final difference Fourier synthesis revealed the presence of two weak peaks in positions that show similar local coordination geometry to fluoride positions from SiO_4F units in other zeolites. These refined successfully as fluoride atoms with occupancies of approximately 10%, although to retain the trigonal bipyramidal geometry of the SiO_4F unit 'same distance' restraints on the fluoride ion oxygen distances were used. The framework structure of SSZ-55 is shown in Figure 2.

The structure of SSZ-55 is particularly interesting in that the crystallographic *c*-axis is very short (~5.12 Å) and it is very unlikely that the SDA, **1**, can fit into the unit cell in this direction. Given this situation there are only a limited number of possibilities: (i) The measured cell is only a subcell, and the real cell is doubled or tripled in the *c*-direction to take account of ordering of the SDA; (ii) The SDA is ordered but is incommensurate with the framework; (iii) The cell is correct, which means that the SDA can show no register between one zeolite channel and the next.

A close look at the frames from the single-crystal X-ray diffraction experiment revealed no evidence for a cell doubling/tripling or incommensurate peaks. Therefore it looks like (iii) is the more likely. Difference Fourier maps reveal a large number of quite intense peaks (maximum 2.8 $eÅ^{-3}$) in channels, whose shape follows the corrugations of the pore structure. Unfortunately, the complex nature of the SDA together with the severe disorder leads to many overlapping areas of electron density in the channels of the material and means that the SDA location could not be unambiguously identified from XRD alone (see below).

However, from this study there are several things we can say about the effect of the SDA and the fluoride on the framework. Most striking are the ADPs on the oxygen atoms surrounding Si2 (Figure 3). These are significantly larger than the other ADPs in the structure, probably indicating that the framework is distorted slightly if there is a fluoride ion connected to it and depending on which of the possible SDA orientations is near to it. X-ray crystallography has been used to confirm the location of fluoride in a number of different zeolites.[13−18,25] However, in previous publications we showed that the local structure of the five-coordinate $[SiO_{4/2}F]^-$ unit in zeolites as determined by XRD did not reflect the true local structure because it was an average between $[SiO_{4/2}F]^-$ and $SiO_{4/2}$ units.[14] This variation from the true local structure is caused by incomplete occupancy of the fluoride ions in the form of either static or dynamic disorder and often leads to the reporting of incorrect Si−F bond distances of between 1.84 and 1.99 Å. However, using solid-state NMR techniques[14] we measured the Si−F bond distance in STF as 1.74 Å which agreed well with predictions made using density functional theory simulations on fluoride ions in SOD and FER frameworks to predict that the $[SiO_{4/2}F]^-$ units are very close to trigonal bipyramidal with Si−F bond distances of between 1.71 and 1.76 Å.[26] The incorrect silicon−fluoride bond distances are a consequence of the X-ray experiment being of insufficient resolution to distinguish the atomic positions of the

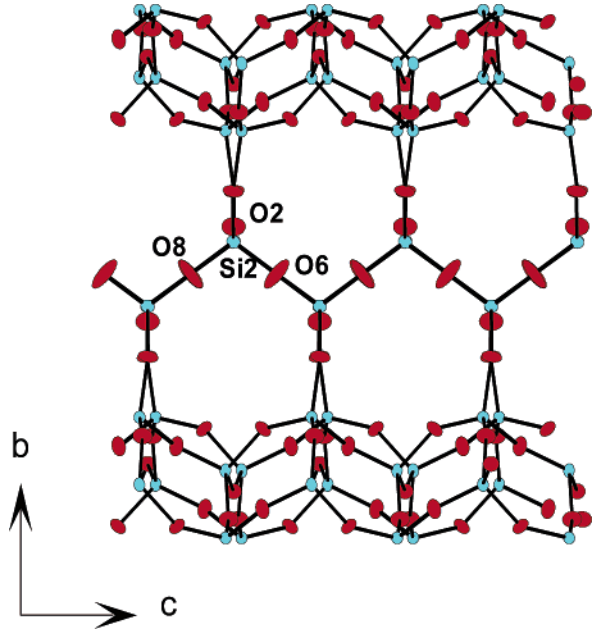

Figure 3. Anisotropic displacement parameters for the silicon and oxygen atoms of SSZ-55 viewed as 50% ellipsoids.

SiO_4 tetrahedra from those of the SiO_4F trigonal pyramid. The two Si−F distances measured here are 1.98(2) and 1.90(2) Å, consistent with the long Si−F distances seen previously.

While the local geometry of the SiO_4F unit is similar to those seen in previous studies the overall fluoride locations in the structure are also of interest as they differ somewhat from those seen on other siliceous zeolite materials. In almost all other crystal structures of fluoride-containing zeolites the fluoride ions are located inside small cages. In several zeolites the fluoride ion is located at the center of a $[4^6]$ cage (i.e., a cage made up of 6 four-membered rings). This arrangement may act to stabilize this type of cage, adding a 'structure-directing' function to the list of possible roles of fluoride in the synthesis of pure silica zeolites. Certainly, this arrangement of fluoride inside $[4^6]$ cages is well-known in aluminum phosphate and gallium phosphate chemistry, and a similar structure-directing influence has been proposed. In the cases of pure silica zeolites NON,[16] STT,[13] and IFR[18] the fluoride ions have been located inside $[4^15^46^2]$, $[4^35^4]$, and $[4^35^26^1]$ cages, respectively. In SSZ-55, however, the fluoride ions are not located in small cages but are attached to silicon atoms of four-membered rings and pointing more or less into the channel spaces. SSZ-55 is a relatively low-density material with thin walls and no cages, and given the fact that fluoride ions usually reside in cages one might consider it surprising that the fluoride route can be used to prepare SSZ-55 at all.

We performed molecular modeling calculations to determine the approximate location of the SDA molecules within the void space of the zeolite framework. During the energy optimization, it became readily apparent that each ring or trimethylammonium group prefers to reside directly above (or below) the large corrugations that encircle the top or bottom parts of the pore structure. The centers of the top corrugations and the centers of the bottom corrugations are displaced about $^1/_2$ *c* or 2.5 Å from each other along the pore axis. Every corrugation can be occupied by either an aromatic ring or trimethylammonium if two molecules are placed in a supercell created by 3 unit cells along the pore axis. The optimal packing occurs when the

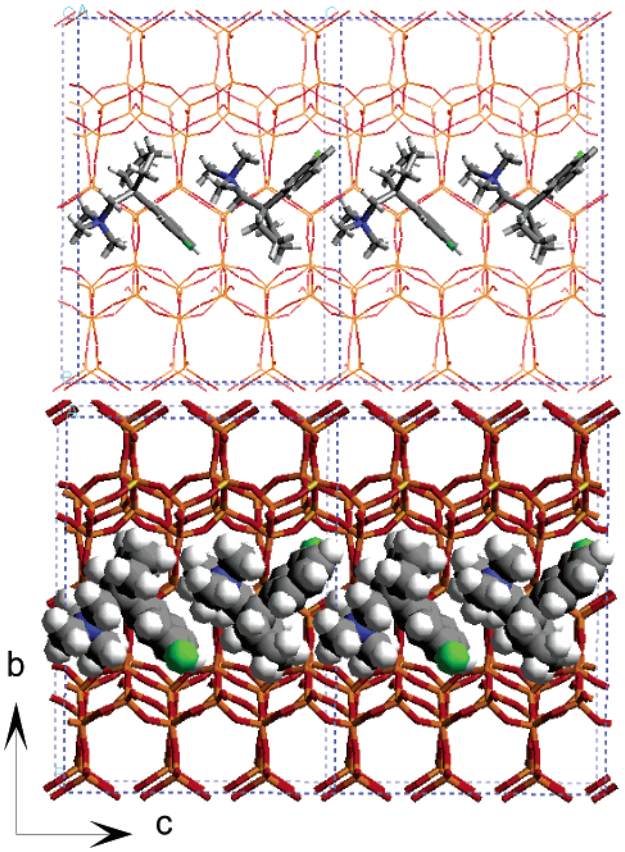

Figure 4. Results of the molecular modeling experiments reveal the most likely positions for the SDAs within the channels of SSZ-55. The top diagram is a stick model of the SDA structure while the bottom is a space-filling model. The tripled unit cell is outlined in dotted lines.

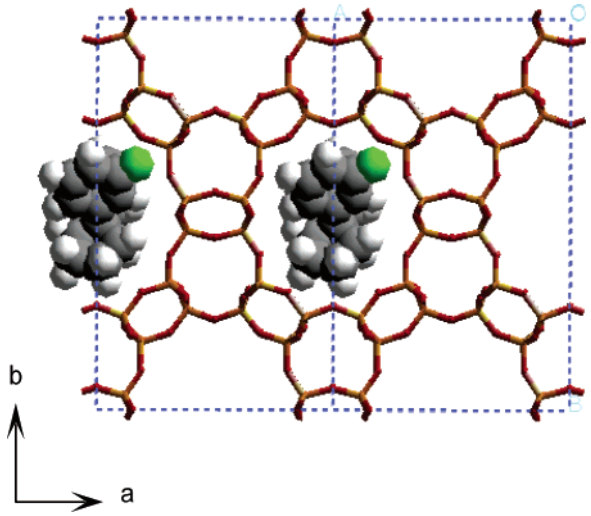

Figure 5. View of the molecular modeling results parallel to the channel direction in SSZ-55 showing the good space-filling properties of this particular SDA.

trimethylammonium group alternates in an up/down fashion along the pore length as shown in the Figure 4.

There is excellent space-filling of the SDA within the pore (Figure 5). According to the above considerations, the best packing occurs with 4 SDA molecules/supercell or 1 SDA/18 Si atoms. From the molecular modeling considerations, we expect about 2 F atoms/18 Si atoms: one fluorine atom from the SDA itself and the other as a charge compensator for the cationic SDA giving an overall molecular formula of $(SiO_2)_{18}F \cdot C_{15}NH_{23}F$. This agrees well with the chemical combustion

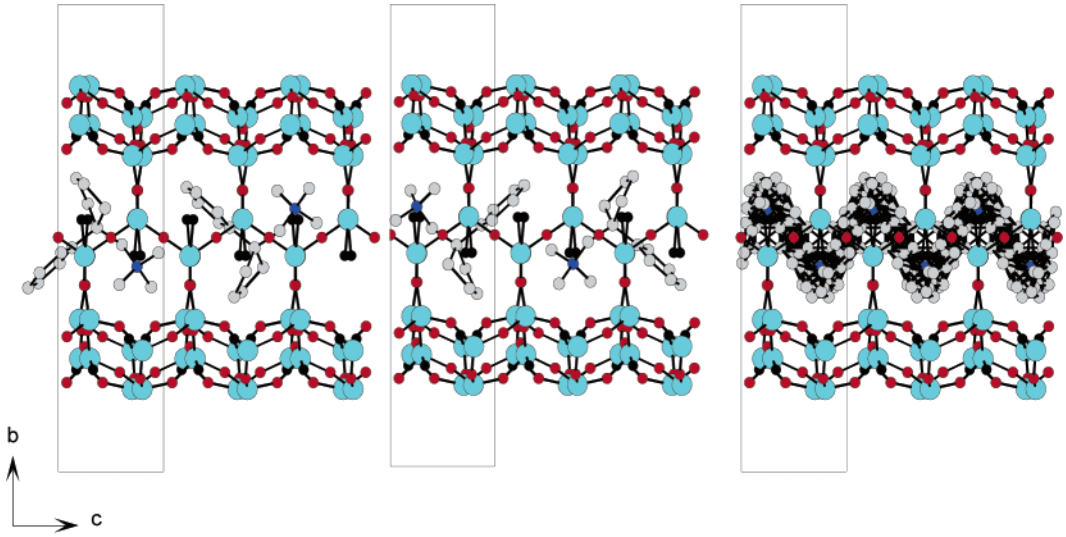

Figure 6. The four possible orientations of the SDA cations (two in the left-hand diagram and two in the center diagram). The average structure (as would be the result of an X-ray diffraction experiment) is shown on the right.

analysis of the organic content of the material: 12.78 wt % for C (calc 13.47), 1.02 wt % for N (calc, 1.05), 1.67 for H (actual, 1.72).

As described above, the charge-compensating fluoride ion can be located using the X-ray diffraction and 1 F atom/18 silicon atoms equates to an occupancy for each of the independent fluorine site of 0.083, which is very close to the free refinement values of ~0.1, remembering that XRD is not an ideal method of accurately quantifying low atomic occupancy factors because of the strong correlation with atomic displacement parameters. In the final cycle of least-squares refinement, the fluorine occupancies were therefore fixed at 0.083. The calculations yielded an optimized energy of about −192 kJ/SDA or −10.7 kJ/mol Si atom. These values indicate highly favorable interactions between the SDA and the framework.

Within an individual pore, the SDA molecules are expected to be ordered with respect to one another for both charge and packing considerations. The current model has the nitrogen atoms as distant from one another as possible. Within a given molecule, switching the locations of any of the rings with the trimethylammonium would result in neighboring trimethylammonium groups, and it would also destabilize the packing arrangement. However, ordering of the SDA molecules between neighboring pores does not seem likely unless the F^- atoms impose long range order on the system. In any case, if there were long range order, then the expected dimension along the pore axis would be $c' = 3c$. However, there was no evidence of the existence of a supercell in the single-crystal data. Therefore, for the average model we used in our single-crystal analysis, we superimposed the positions of the two molecules within a single unit cell, making sure that the total occupancy summed to 4/3 molecule/conventional unit cell.

Taking into account the head to tail ordering and the two possible orientations with these SDA chains (left to right and right to left) means that there are actually four possible SDA orientations in each of the unit cells (Figure 6). Taking into account the pore-filling results described above, if all orientations are equally likely then the resulting average structure as seen in the results would have a large number of atoms with an occupancy factor of ~0.1667. This means a scattering power of ~1 $eÅ^{-3}$, consistent with the magnitude of the difference Fourier peaks remaining in the channel volume. Indeed the first 10 Fourier peaks match atomic positions relatively well with those we would expect from the average structure based on the modeled SDA positions. Unfortunately, many of the remaining atom positions overlap so closely that a free refinement of the SDA position using XRD is unrealistic. However, the results of the molecular modeling do provide what seem to be very plausible SDA positions, and inclusion of the template electron densities with fixed atomic positions and displacement factors does improve the overall refinement slightly. Using the program Squeeze, which removes the contribution to the X-ray scattering from the atoms in the channels, leads to a significant improvement in the *R*-factors for the refinement ($R_1 = 0.0394$). The program Squeeze indicates a total of 178 electrons per unit cell in the 443.1 $Å^3$ of SDA-accessible area in the channels in the structure. This agrees remarkably well with the loading of 1.33 SDAs per unit cell, which totals 172 electrons per unit cell, confirming that the molecular modeling is producing a physically reasonable result.

We also examined the interactions of the SDA with other all-silica, one-dimensional 12-ring zeolite frameworks including MTW, GON, SSZ-31, SSY, and AFI. In some cases there was insufficient space within the pores to yield a negative stabilization energy. The next closest stabilization was determined for AFI, and this energy was less than half that calculated for the SSZ-55 framework. It is worth noting that SSZ-55 (ATS) has the most open framework among one-dimensional 12-ring zeolites (17.0 T atoms/1000 $Å^3$) and that SSZ-24 has the second most open framework. If the F atom of the SDA is placed in the para position rather than the meta, the SDA is instead selective for the 14-ring zeolite SSZ-53. Interestingly, although the pore dimensions are larger in SSZ-53, it possesses a higher framework density than SSZ-55.

In conclusion, the single-crystal structure of as-made SSZ-55 reveals that the overall structure of the material is clearly non-centrosymmetric despite the fact that the topological (highest possible) symmetry of the framework is centrosymmetric. In addition, this material crystallizes in a different spacegroup to others with the same framework connectivity. The reasons for these changes in symmetry are not entirely obvious. However, it seems likely that the interplay between the localized negative charges on the fluoride ions attached to the silicon atoms of the framework and the positively charged organic structure-directing agent play an important role in determining the final symmetry. Certainly the sites where

fluoride ions are found in this material are unusual for silica-based zeolites. It is important to note that the pure silica version of SSZ-55 cannot be prepared in the absence of fluoride ions, indicating the importance of extraframework negative charge such as that supplied by fluoride in the crystallization of these materials. In this case, the location of the SDA is complicated by the fact that the unit cell is not large enough in one direction, and so the SDA is necessarily disordered. However, molecular modeling has given some insight into likely local structure around the SDA.

Acknowledgment. R.E.M. thanks the Royal Society for the Provision of a University Research Fellowship. We thank Dr. Manfred Buck for help with the SHG measurements. We thank Saleh Elomari at Chevron, the inventor of the SSZ-55 material, for supplying us with the SDA used in this work. Also Tom Rea at Chevron is to be thanked for the microscopy work.

Supporting Information Available: Crystallographic information files (CIF) are available for the structure of SSZ-55 as well as ^{13}C MAS NMR and ^{19}F NMR spectra of SSZ-55. This material is available free of charge via the Internet at http://pubs.acs.org.

References and Notes

(1) (a) Davis, M. E. *Nature* **2002**, *417*, 813. (b) Wheatley, P. S.; Butler, A. R.; Crane, M. S.; Fox, S.; Xiao, B.; Rossi, A. G.; Megson, I. L.; Morris, R. E. *J. Am. Chem. Soc.* **2006**, *128*, 502.

(2) Flanigen, E. M.; Patton, R. L. U.S. Patent No. 4073865, 1978.

(3) Morris, R. E.; Burton, A.; Bull, L. M.; Zones, S. I. *Chem. Mater.* **2004**, *16*, 2844.

(4) Camblor, M. A.; Villaescusa, L. A.; Diaz-Cabanas, M. J. *Top. Catal.* **1999**, *9*, 59.

(5) Kuperman, A. S.; Oliver, S.; Ozin, G. A.; Garces, J. M.; Olken, M. M. *Nature* **1993**, *365*, 239.

(6) Corma, A.; Rey, F.; Rius, J.; Sabater, M. J.; Valencia S. *Nature* **2004**, *431*, 287.

(7) Corma, A.; Díaz-Cabañas, M. J.; Joaquín Martínez-Triguero, J.; Rey, F.; Rius, J. *Nature* **2002**, *418*, 514.

(8) Paillaud, J. L., Harbuzaru, B., Patarin, J. Bats, N. *Science* **2004**, *304*, 990.

(9) Barrett, P. A.; Camblor, M. A.; Corma, A.; Jones, R. H.; Villaescusa, L. A. *J. Phys. Chem. B* **1998**, *102*, 4147.

(10) Zones, S. I.; Darton, R. J.; Morris, R. E.; Hwang, S.-J. *J. Phys. Chem. B.* **2005**, *109*, 652.

(11) Koller, H.; Wolker, A.; Eckert, H.; Panz, C.; Behrens, P. *Angew. Chem., Int. Ed Engl.* **1997**, *36*, 2823.

(12) Koller, H.; Wolker, A.; Villaescusa, L. A.; Diaz-Cabanas, M. J.; Valencia, S.; Camblor, M. A. *J. Am. Chem. Soc.* **1999**, *121*, 3368.

(13) Camblor, M. A.; Diaz-cabanas, M. J.; Perez-Pariente, J.; Teat, S. J.; Clegg, W.; Shannon, I. J.; Lightfoot, P.; Wright, P. A.; Morris, R. E. *Angew. Chem., Int. Ed Engl.* **1998**, *37*, 2122.

(14) Fyfe, C. A.; Brouwer, D. H.; Lewis, A. R.; Villaescusa, L. A.; Morris, R. E. *J. Am. Chem. Soc*. **2002**, *124*, 7770.

(15) Caullet, P.; Guth, J.; Hazm, J.; Lamblin, J.; Gies, H. *Eur. J. Solid State Inorg. Chem.* **1991**, *28*, 345.

(16) Van de Goor, G.; Freyhardt, C. C.; Behrens, P. *Z. Anorg. Allg. Chem.* **1995**, *621*, 311.

(17) Villaescusa, L. A.; Wheatley, P. S.; Bull, I.; Lightfoot, P.; Morris, R. E. *J. Am. Chem. Soc.* **2001**, *123*, 8797.

(18) Bull, I.; Villaescusa, L. A.; Teat, S. J.; Camblor, M. A.; Wright, P. A.; Lightfoot, P.; Morris, R. E. *J. Am. Chem. Soc*. **2000**, *122*, 7128.

(19) (a) Cox, S. D.; Gier, T. E.; Stucky, G. D.; Bierlein, J. *J. Am. Chem. Soc.* **1988**, *110*, 2986. (b) Cox, S. D.; Gier, T. E.; Stucky, G. D. *Chem. Mater.* **1990**, *2*, 609. (c) Marlow, F.; Wubbenhorst, M.; Caro, J. *J. Phys. Chem.* **1994**, *98*, 12315−12319. (d) Reck, G.; Marlow, F.; Kornatowski, J.; Hill, W.; Caro, J. *J. Phys. Chem*. **1996**, *100*, 1698.

(20) Hulliger, J.; Roth, S. W.; Quintel A.; Bebie, H. *J. Solid State Chem.* **2000**, *152*, 49.

(21) See Meier, W. M.; Olson, D. H.; Baerlocher, C. *The Atlas of Zeolite Structure Types*; Elsevier: New York, 1996 or at www.iza-online.org for a description of zeolite topologies.

(22) Smith, J. V.; Pluth, J. J.; Andries, K. J. *Zeolites* **1993**, *13*, 166.

(23) (a) Wu, M. G.; Deem, M. W.; Elomari, S. A.; Medrud, R. C.; Zones, S. I.; Maesen, T.; Kibby, C.; Chen, C.-Y.; Chan, I. Y. *J. Phys. Chem. B.* **2002**, *106*, 264. (b) Elomari, S. A.; Zones, S. I. *Proc. 13th Int. Zeolite Conf.* **2001**, 03-O-03.

(24) Borecka-Bednarz, B.; Bree, A. V.; Patrick, B. O.; Scheffer, J. R.; Trotter, J. *Can. J. Chem.* **1998**, *76*, 1616

(25) Attfield, M. P.; Weigel, S. J.; Taulelle, F.; Cheetham, A. K. *J. Mater. Chem.* **2000**, *10*, 2109.

(26) Attfield, M. P.; Catlow, C. R. A.; Sokol, A. A. *Chem. Mater*. **2001**, *13*, 4708.